Aerodynamic Drag and Stability Characterisation of a Rigid Parachute

Teo Ci En Teresa[1], Low Enya[2], Lee Jian Ming[3]

Cedar Girls' Secondary School[1], Singapore Chinese Girls' School[2], DSO National Laboratories[3]

1. Abstract

This paper consists of a series of research done on unmanned parachutes by using a Computer Aided Design (CAD) software as well as Computational Fluid Dynamic (CFD) simulations. It makes use of data from such tools as well as results from testing prototypes to conclude the stability and drag force experienced by the parachute. The paper also explains the research done when choosing the size and materials used to make the prototype. While the results from the parachute modeled in the CFD software were ideal, it lacks consideration of external factors faced during the actual testing such as the parachute being affected by wind. Hence, data from testing the prototype is presented as a more realistic value as it takes into consideration these external factors.

2. Math formulas

$$D = F_z \cos\Theta + F_x \sin\Theta$$

where:

D = drag force experienced by parachute

F_z = force experienced by parachute in the z-axis direction

F_x = force experienced by parachute in the x-axis direction

Θ = angle of attack of the force

$$A_p = \frac{2gm}{\rho C_D v^2} \text{ [1]}$$

where:

A_p = surface area of parachute canopy

G = the acceleration due to gravity, 9.81 m/s^2 at sea level

m = the mass of the prototype

ρ = the density of air at sea level (1.225 kg/m^3)

C_D = the coefficient of drag of the parachute

v = the descent velocity of the prototype

$$C_D = \frac{Fd}{0.5\rho v^2 s}$$

Where:

C_D = Coefficient of drag

F_D = drag force experienced by parachute

ρ = the density of air at sea level (1.225 kg/m^3)

v = velocity of prototype

s = area of parachute canopy

3. Introduction

Parachutes can be considered one of the easiest ways to reduce a payload's velocity safely. There are different types of parachutes – manned (Fig. 3.1) and unmanned parachutes (Fig. 3.2). Parachutes are required to be resistant to the environment and able to withstand different operating conditions. They are also required to have a reasonable balance between improving drag and maintaining stability.

Fig. 3.1: manned parachute

Fig. 3.2: unmanned parachute

This paper will focus on the unmanned parachute. A few key advantages would be the fact that they can be deployed in and withstand harsh weather conditions, are cheaper, and have no need for carrying human necessities such as food and water. Thus, some examples where it can be used are for providing food aid to a country or an area facing a crisis.

The flight of the parachute can be affected by many different factors, such as mass of payload, area of parachute, or length of string, etc. This study aims to characterise the aerodynamic drag and stability of a rigid parachute using simulations and prototype testing. It will elaborate on the

methods used to design the parachute and the measurements used when creating it. It also details the experiments carried and the results used to confirm a proposed unmanned parachute.

4. Literature review

Research was done on past published papers so as to gain a deeper and wider understanding of the specifics of how an unmanned parachute should be built and calibrated.

An estimation method for parachute parameters mentioned in [2] allowed us to understand how different shapes of the parachute affected the descent. As the shape of the parachute that they used was similar to what was going to be used for ours, it was very helpful in giving us more insight on the pros and cons of each shape. This allowed us to make more informed decisions on the size and shape of the parachute. Additionally, the project also used a Computational Fluid Dynamics (CFD) software which guided us when running our own CFD software.

Parachute Dynamic Stability and the Effects of Apparent Inertia by Jason M. Ginn, Ian G. Clark and Robert D. Braun [3] allowed us to explore how the surrounding atmosphere affects the inertia of the parachute, and how this in turn causes the parachute to differ in stability. This paper offered insights as to how the inertia value was determined as well as the corresponding velocity and angle of attack of the parachute. The density was also varied and the stability was then recorded for each value of the changed variable. This paper was useful in giving us insights as to how we could build a more stable parachute and to ensure the best design for it.

Parachute-Payload System Flight Dynamics and Trajectory Simulation by Giorgio Guglieri [4] expands more on the topic of airflow through and around the parachute and how this causes the stability and deceleration to change. In the paper, a model of the parachute and payload was made, using its acceleration, mass, flight path angle and other factors to determine the drag force of the parachute. A simulation software was also used to model the parachute-payload system to achieve data from flight tests. The formulas used in this paper were useful in helping us determine values for our parachute.

The book Parachute Recovery Systems: Design Manual written by Theodor W. Knacke [5] is a detailed guide on how to navigate parachute recovery systems. It gives users the means to assess, choose, develop, test, and produce parachute recovery systems. These systems comprise equipment for impact attenuation, flotation, recovery and range from straightforward, single-parachute assemblies to multiple-parachute systems. The selection of the best recovery system idea, a computerized method for measuring parachute performance, force and stress analysis, geometric gore design, component layout, material selection, system design, manufacturing, and in-service maintenance are only a few of the topics covered. This book was beneficial in giving us an idea of how to plan for any unforeseen complications.

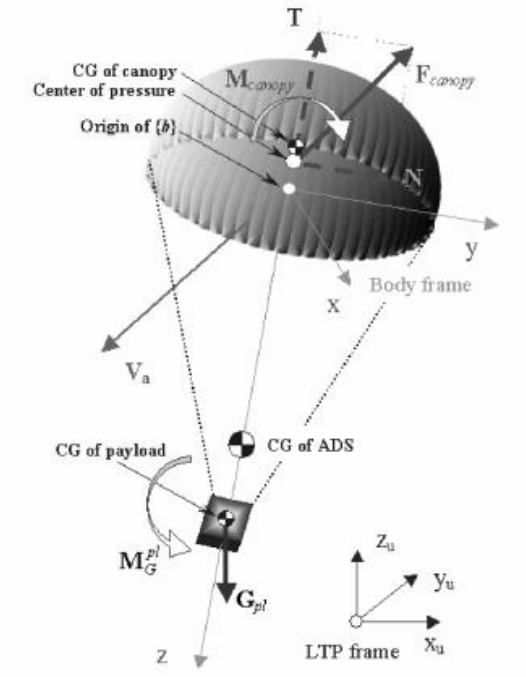

Fig. 4: Free body diagram of a parachute [6]

Six-Degree-of-Freedom Model of a Controlled Circular Parachute [6] is a detailed paper explaining the different and numerous forces that act on the parachute during descent. Through this paper, one can come to understand that the total force that is acting on the parachute can be determined by the force acting in the direction of the z-axis, the force acting in the direction of the x-axis, as well as the angle of attack, using the formula of $D = F_z cos\,\theta + F_x sin\,\theta$.

5. Methodology

Literature review was first performed to gain a better understanding of the overall structure and design of parachutes. This was done to find out the different formulas that were needed to calculate the parachute area, mass of the parachute and payload and also the coefficient of drag. This was particularly important as it would be a key foundation to how the choosing of materials would be done as well as the shape and structure of the parachute, making sure that it could be as accurate and precise as possible so that the parachute could be as secure and stable as possible before its first test.

The software SolidWorks was used to draw the Computer Aided Design (CAD) geometry of our parachute designs and payload. We created many geometries of parachutes with different hole diameters at the top ranging from 0.05m to 0.3m in intervals of 0.05m. The simulations would allow us to compare the net force of the parachutes and conclude the best hole size to use on our actual prototype. We also conducted simulations of the different parachutes using different velocities and angle of attacks. This allowed our results to simulate different operating conditions of the parachute so that we could accurately compare the different results to conclude the size of our final prototype.

CFD and a physical testing of the parachute would be conducted to obtain our results.

ANSYS was the CFD software of choice as it is a reputable and reliable software used widely for engineering simulations. CFD was used to obtain quicker lower-fidelity results. This will then be complemented with the flight test of the parachute to be validated. A geometry of the parachute was created using ANSYS Workbench Fluent.

As we had estimated a payload of around 100g, we concluded through the formula $A_p = \frac{2gm}{\rho C_d v^2}$ that we needed to have a parachute with a diameter of 1.4m. The diameter of the hole of the parachute was determined through literature reviews.

The physical testing will be performed by releasing a parachute at a higher altitude and using an IMU to measure the 6 degrees of freedom of the parachute during descent. The payload Fig 11.12 was drawn as a CAD which consisted of the Inertial Measurement Unit (IMU) and some weights that were held in a 3D printed box. We also created 6 small holes along the sides and the lid each so that we could secure the lid to the box and the payload to the parachute. The dimensions for the box was 80mm by 60mm by 50mm. This CAD was then used as a model that was uploaded onto the 3D printer. As we calculated a mass of 125g for the size and speed of the parachute, additional Blu Tack was used as extra weight given that the IMU and box itself were not heavy enough to fulfill the mass criteria.

Additionally, online research was also done on the different parts of the parachute and payload that was to be assembled and improved on. We had to find motherboards, an IMU, batteries and wires. This IMU [7] was chosen in the end as it was one that was compact enough to save space and had Bluetooth connection, a chargeable battery inside as well as memory, which meant that only the IMU was needed.

The length of the string was determined by the diameter of the parachute. Literature review [8] suggested that parachute shroud lines should be 115% of the diameter length. Since our parachute had a 1.4m radius, our shroud lines were 1.61m. The chosen material for the string was fishing line. The fishing line had a diameter of 0.5mm and could hold up to 35 pounds. It was chosen as it could withstand heavy weights and was durable.

We first made a paper prototype Fig. 11.8 that was of a scaled area of 1:25. This prototype was conically shaped with a small hole of radius 0.5cm cut at the top to allowed the relief of pressure, where Blu Tack was used as a payload. Since this prototype was made out of paper, it was very sturdy and inflexible which we realised when we dropped it, affected the stability during descent. This resulted in the parachute tipping and tilting to one side, eventually tipping the parachute over and making it collapse during its descent. Due to the tape being heavy and the parachute shape not being symmetrical, it tends to tilt to one side and roll. We also discovered that the density of the paper was too heavy compared to the actual cloth that was going to be used. We then decided to change the material of the parachute.

For the second prototype Fig 11.9 it was decided to use plastic as it was a lightweight and flexible material that would be capable of trapping more air during descent. The shape of this parachute was also conical and it had a scaled area of 1:8 with the actual one that was going to be created. However, our supervisor told us that this parachute was not of the correct shape, that it would not open fully if the weight was not heavy enough and the cross-sectional area of the parachute would

keep changing when the weight changed. He suggested that we try to build a prototype with a hemispherical shape [9] rather than a conical one to increase stability during descent.

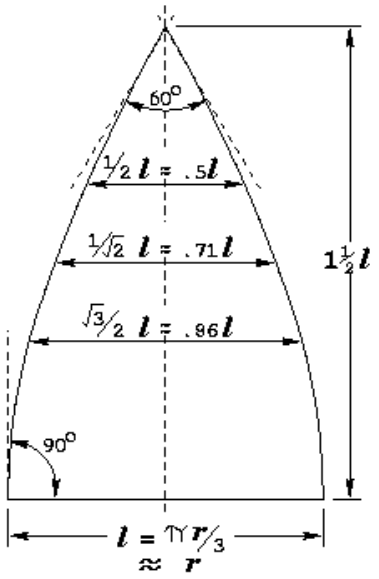

Fig. 5: diagram of 1 of 6 panels of parachute prototype [9]

Our third prototype Fig 11.10 was a plastic parachute with a hemispherical shape, of a scaled area of 1:8 of the actual parachute and we used a weight of 25g in Blu Tack and the link above to calculate the shape of the 6 sides of the parachute that was cut out. Fig. 5 shows the formulas we used to measure the perfect shape we needed to cut out to make the canopy hemispherical. We then taped the sides of the parachute together, trying to use the same amount of tape every time so that the parachute would be as geometrically similar as possible. This would make it more stable during the descent. During testing, we dropped the parachute from the second level while one of us watched it go down from the staircase. This would ensure that we could see the parachute's journey down from different angles so as to identify areas that need improving from different perspectives.

The last prototype Fig. 11.11 was a 1.4m diameter parachute that was made out of nylon ripstop fabric. This material was chosen as nylon is used very commonly to make parachutes as it is a very durable material. Ripstop means that the fabric is woven together so this would mean that the material is stronger while still being flexible. This prototype had a hole at the top of the it so as to allow for the pressure in the hemisphere to escape. The hole was of a diameter of 0.35m. The hole was of 1:5 area of the parachute. This hole size was chosen as literature reviews explained that a 20%-hole size of the whole parachute was the optimum ratio as this would allow for a stable descent of the parachute.

The experiment was performed from a 5-story carpark deck with an estimated height of 20 meters.

6. Results

Results were gathered from both the CFD and the IMU from experimental testing. Experimental testing was conducted for 3 successful descent and the results were averaged out. Data regarding Coefficient of Drag against velocity which would characterise Aerodynamic drag was collected and plotted. Angles regarding X and Y axis (Pitch and Roll) were recorded and plotted over time which would be an indicator of parachute stability during descent.

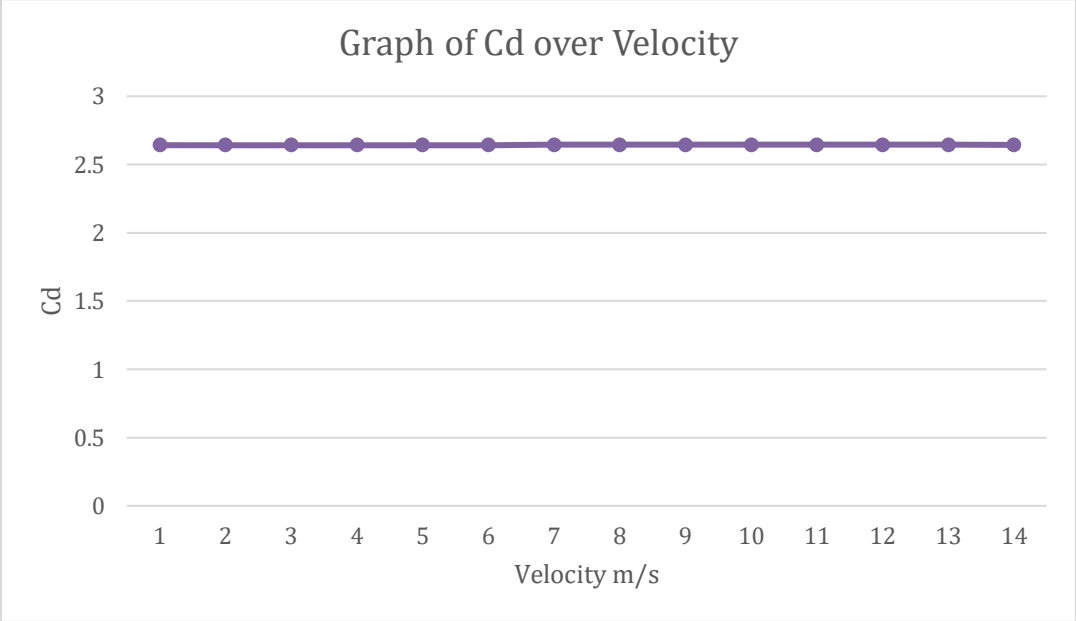

Fig. 6.1.1 : CFD graph of Cd over Velocity

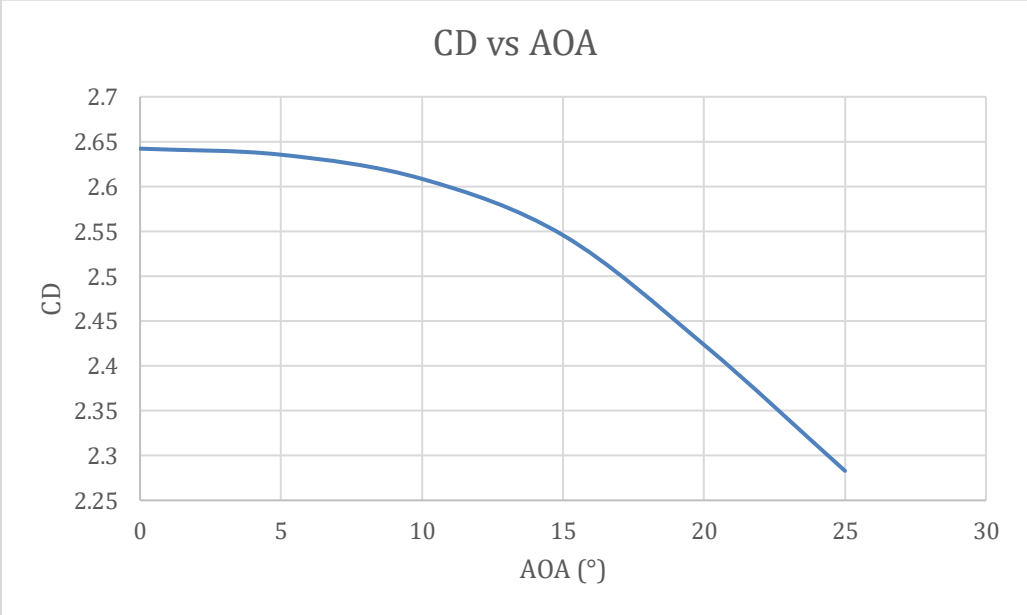

Fig 6.1.2 : CFD graph of Cd over AOA

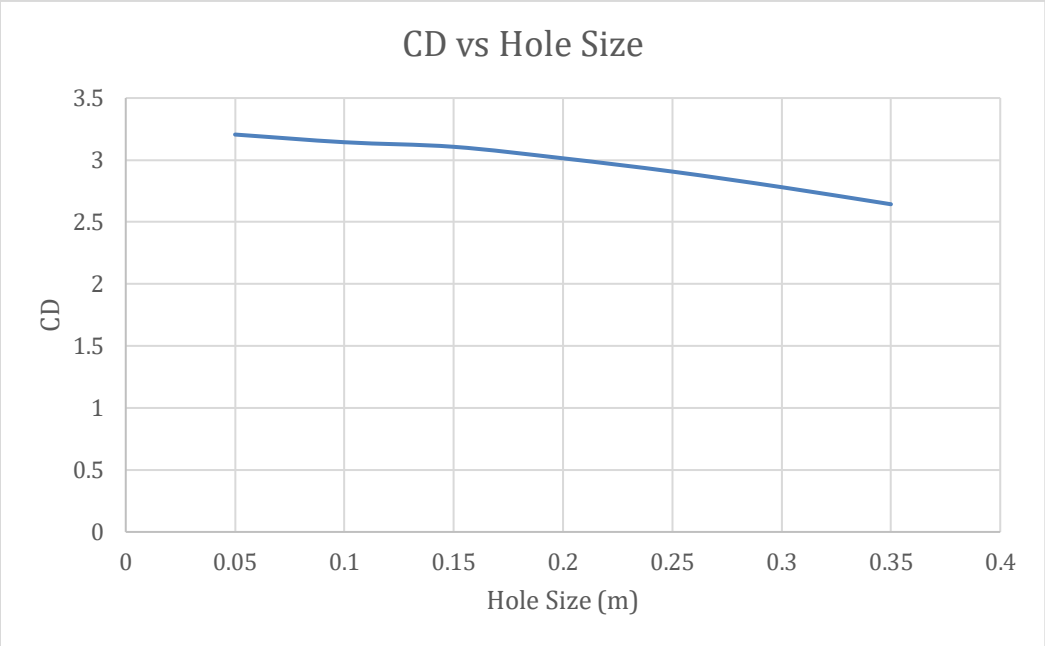

Fig. 6.1.3 : CFD graph of Cd over Hole Size

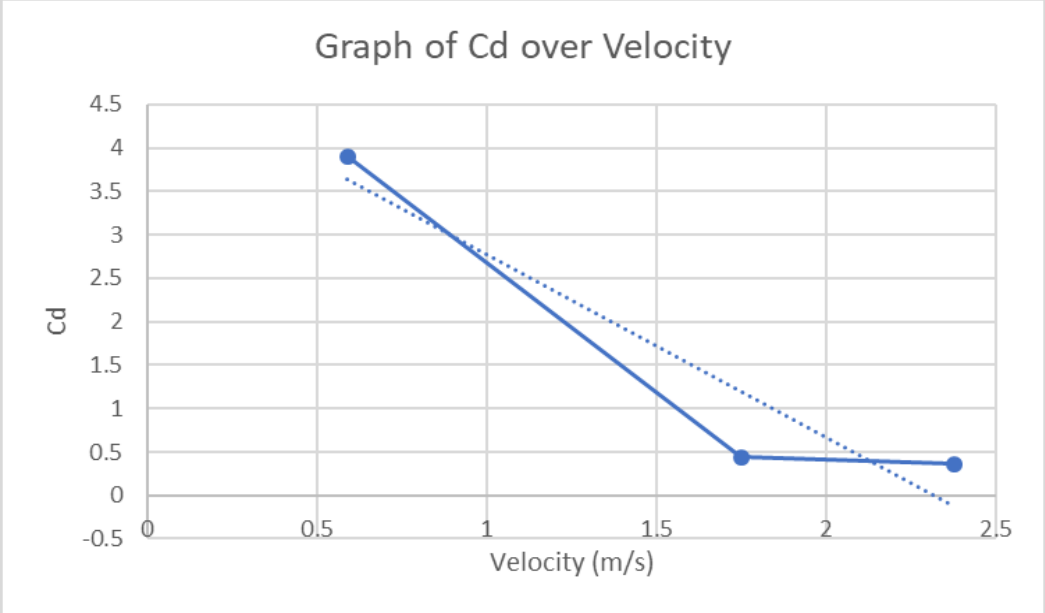

Fig. 6.2: Experimental testing Graph of C_D over Average velocity from each of the three tests were taken and plotted with their respective Cd and a best fit line was also plotted.

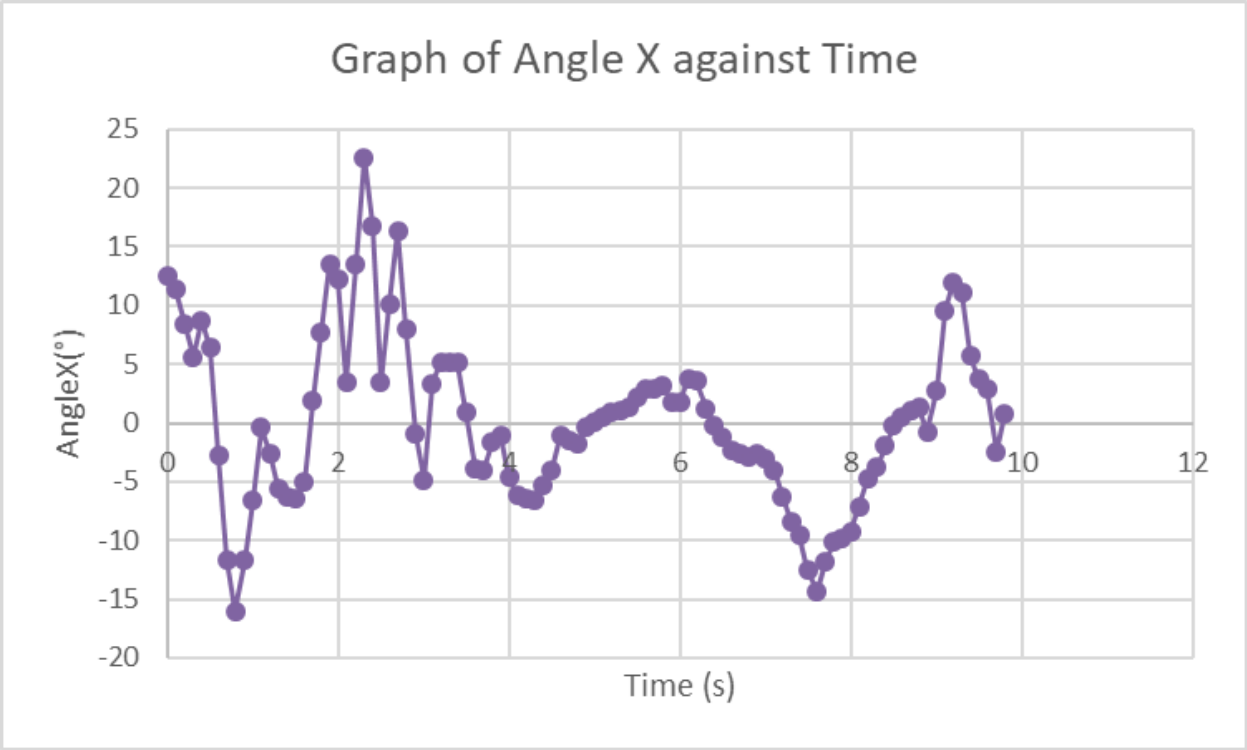

Fig. 6.3: Experimental testing Graph of Angle X (Pitch) over Time

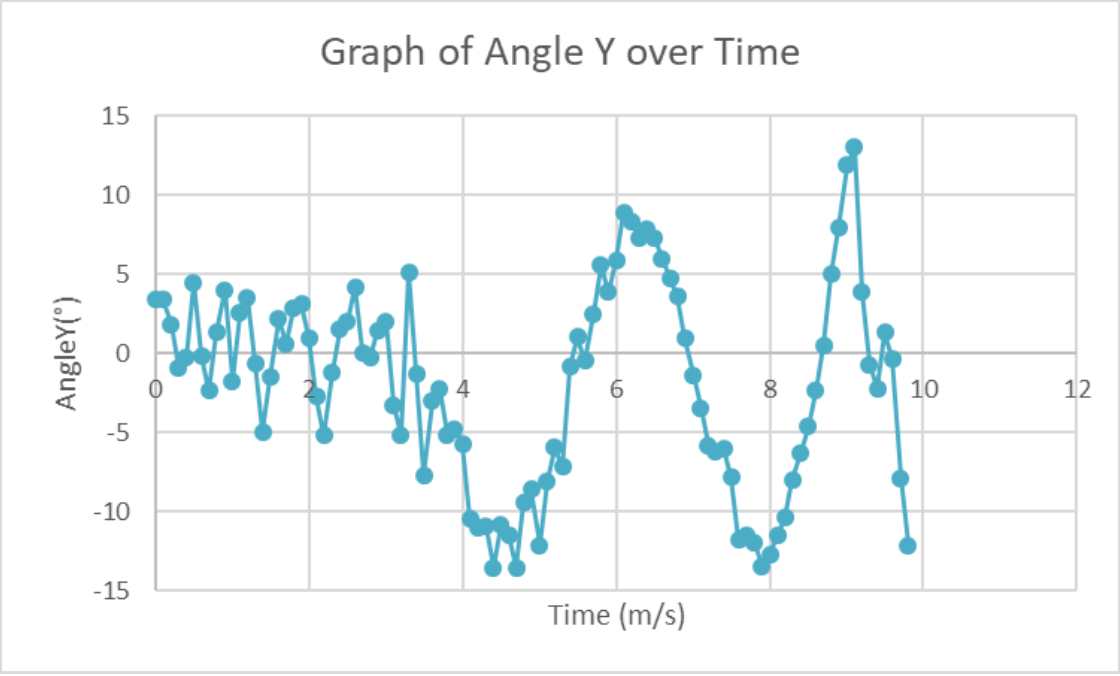

Fig. 6.4: Actual testing Graph of Angle Y (Roll) over Time

7. Discussion

The coefficient of drag (C_D) of the parachute Fig. 6.1.1 in the simulation was negligible fluctuations of not more than 0.0025. It can hence be concluded that the drag force is proportional to the velocity at which the parachute is descending. The drag coefficient can be seen to have an inversely proportional relationship to the angle of attack, which can be seen in Fig 6.1.2. This is expected as there is less flow orthogonal to the parachute which results in a lower force and drag. The drag coefficient is also seen to decrease the as the hole size of the parachute increases. This is also expected as there is more air that is escaping the parachute and the effective area of the parachute decreases. This results in a lower upwards force on the parachute and a lower drag.

The results of the experimental testing between the relationship of C_D and velocity from Fig 6.2 see a downward trend unlike in Fig 6.1.1. Theoretically, Fig 6.1.1 and Fig 6.2 should be generally the same. However, from Fig 6.2 it can be concluded that the drag force increased at a slower rate than the velocity. These results can be explained by the external forces acting on the parachute during testing, such as wind. The wind would have pushed the parachute to drift and this affected the resultant force that acted on the parachute. Results in Fig 6.1.1 are of an ideal situation where there are no external disturbances during testing. Additionally, the CFD model was of a solid form and constant wetted area, unlike the actual prototype made from a flexible cloth which allowed for the wetted area to change in relation to drag force and this affected and varied the C_D. Hence the results in Fig 6.1.1 and Fig 6.2 vary.

In Fig. 6.3, Pitch shows greater variations in the first three seconds, proving that the payload box is unstable. This is due to the fact that the parachute has not opened fully, thus causing the forces to fluctuate and the box to shake. After the third second, the parachute opens fully and falls at a steady speed, allowing the payload to stabilize, hence the angle has lesser fluctuates of not more than 15 degrees in either direction. Furthermore, the angle is oscillating around 0° of deflection, which shows its stability as it tends to return to its equilibrium state.

As shown in Fig. 6.4, Roll fluctuates much less than Pitch for the first three seconds, which expresses that the forces acting in the Y-axis direction were much less compared to those acting in the X-axis direction, perhaps due to wind pushing on the side of the box. When the parachute fully opens after the third second, the opposite is seen on the graph, and Pitch fluctuates more than Roll. This could be accounted to the sudden increase in the drag force caused by the parachute opening, which in turn causes the payload to have a sudden decrease in speed. This might cause the payload to jerk and rotate, hence the force of the wind now acts on the other side of the box, explaining why it now rotates in a different direction. Fortunately, this fluctuation of Pitch only has a maximum of 15 degrees on either direction.

Hence it can be established that the parachute is stable during descent. Whereby aerodynamic drag in realistic situation will increase at a slower rate compared to velocity unlike in the CFD where aerodynamic drag is proportional to speed.

8. Conclusion

It can be concluded that testing of the project is not of an ideal situation as the experiment had external disturbances during descent such as wind. Unfortunately, it could not be rectified under the circumstances and resources given. However, when compared with the CFD results the

conclusion can be drawn that a hemispherical parachute with a hole diameter 20% that of the parachute at the top is stable enough for unmanned descent with allowance for minor disturbances, further proven through the results in the graph. Future investigations can be conducted in a more controlled environment such as tunnel testing which would reduce external disturbances giving more accurate data.

9. Acknowledgments

We wish to acknowledge the generous support and insights given by our mentor, Lee Jian Ming and our co-mentor, Amos Wong, from the Guided Systems (GS) department in DSO National Laboratories.

10. References

[1] The Mathematics of Flat Parachutes (pg 2) formula of relationship between area of parachute and mass of payload

By: Brohm, J.R. (2004, September 4). *The Mathematics of Parachutes*. Sunward. Retrieved November 21, 2022

The Mathematics of Parachutes (sunward1.com)

[2] Journal of Physics: Conference Series - An estimation method for parachute parameters

Citation: Zhibin Li et al 2021 J. Phys.: Conf. Ser. 1786 012012

[3] Parachute Dynamic Stability and the Effects of Apparent Inertia by Jason M. Ginn, Ian G. Clark and Robert D. Braun

[4] Parachute-Payload System Flight Dynamics and Trajectory Simulation by Giorgio Guglieri

[5] Parachute recovery systems design manual

Cite: theo W. knake contractor for the recovery systems division Aerosystems department

[6] Journal of Aircraft Vol. 40, No. 3, may-June 2003 - six0Cegree-of-freedom Model of a controlled circular parachute

Citation: Vladimir N. Dobrokhodov,¤ Oleg A. Yakimenko,† and ChristopherJ. Junge‡

[7] WITMOTION Inertial Measurment Unit Sensor

[Bluetooth 5.0 Accelerometer+Inclinometer] WT901BLECL MPU9250 High-Pre – WitMotion (witmotion-sensor.com)

[8] Fruity Chutes: How to make a Parachute

https://fruitychutes.com/help_for_parachutes/parachute-help/how_to_make_a_parachute.htm

[9] Kiteplans: Hemisphere Parachute Design

Hemisphere Parachute Design (kiteplans.org)

Appendix

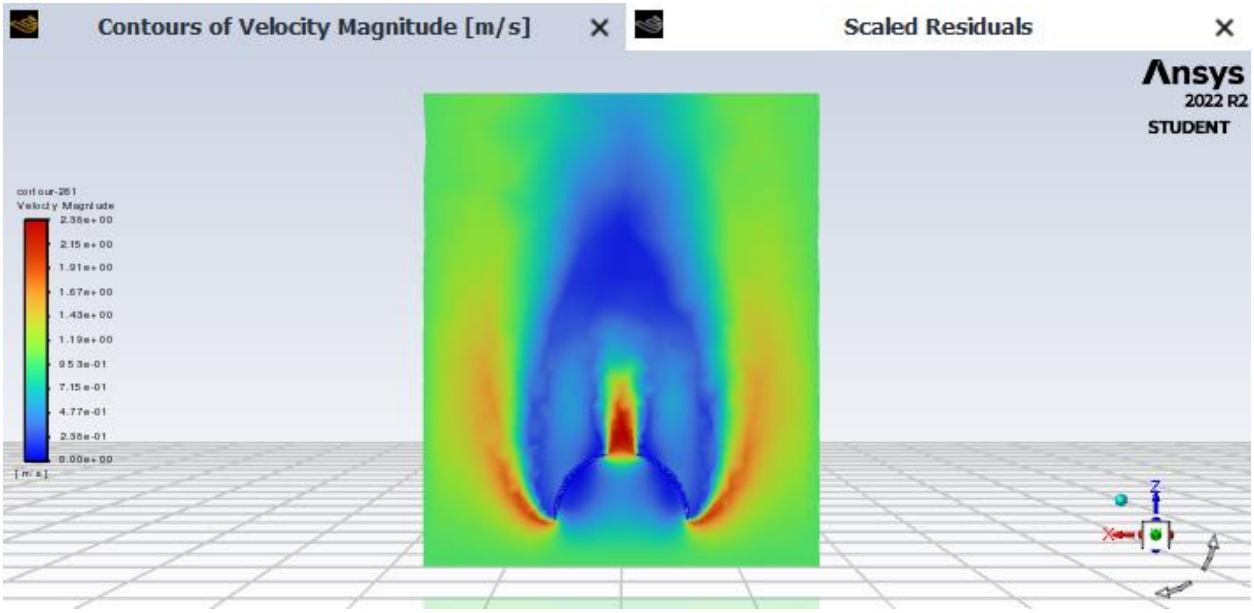

Fig. 11.1: Velocity contour of parachute vertically upright, hole size of 0.35m, falling at a terminal velocity of 1m/s

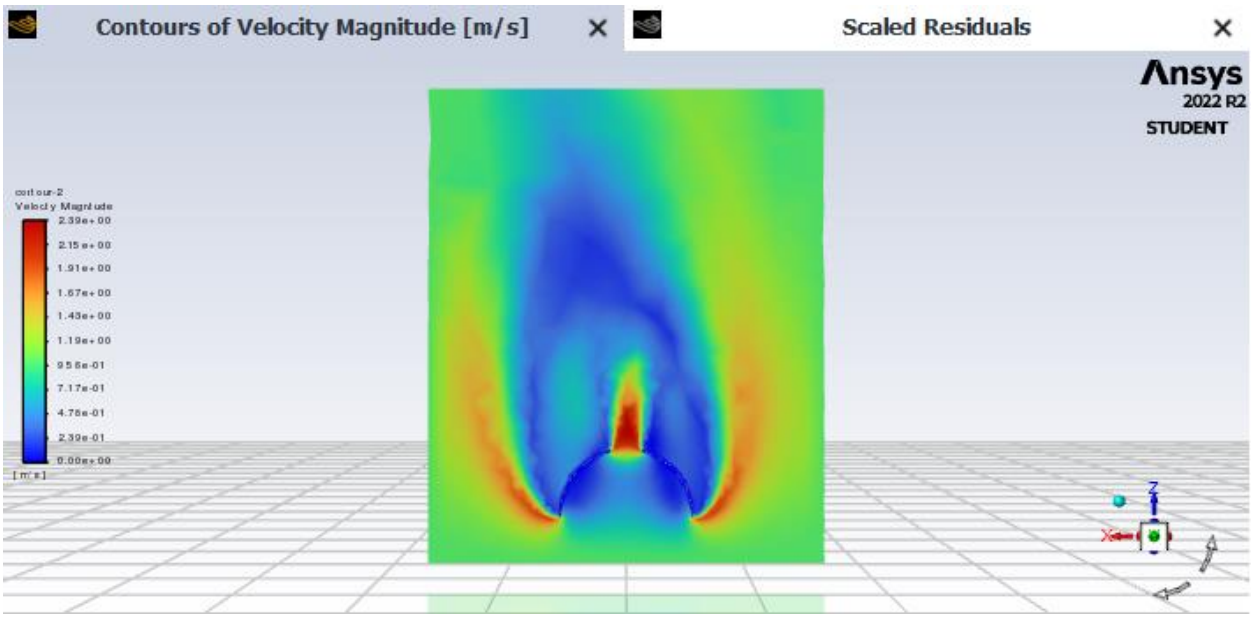

Fig. 11.2: Velocity contour of parachute tilted 5 degrees, hole size of 0.35m, falling at a terminal velocity of 1m/s

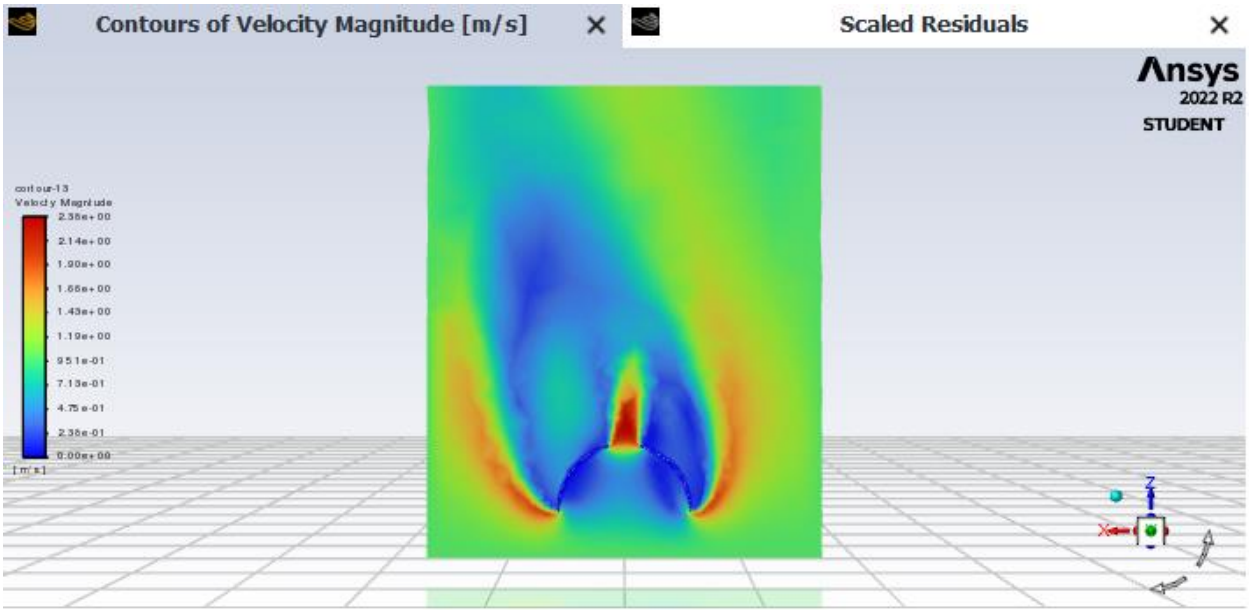

Fig. 11.3: Velocity contour of parachute tilted 10 degrees, hole size of 0.35m, falling at a terminal velocity of 1m/s

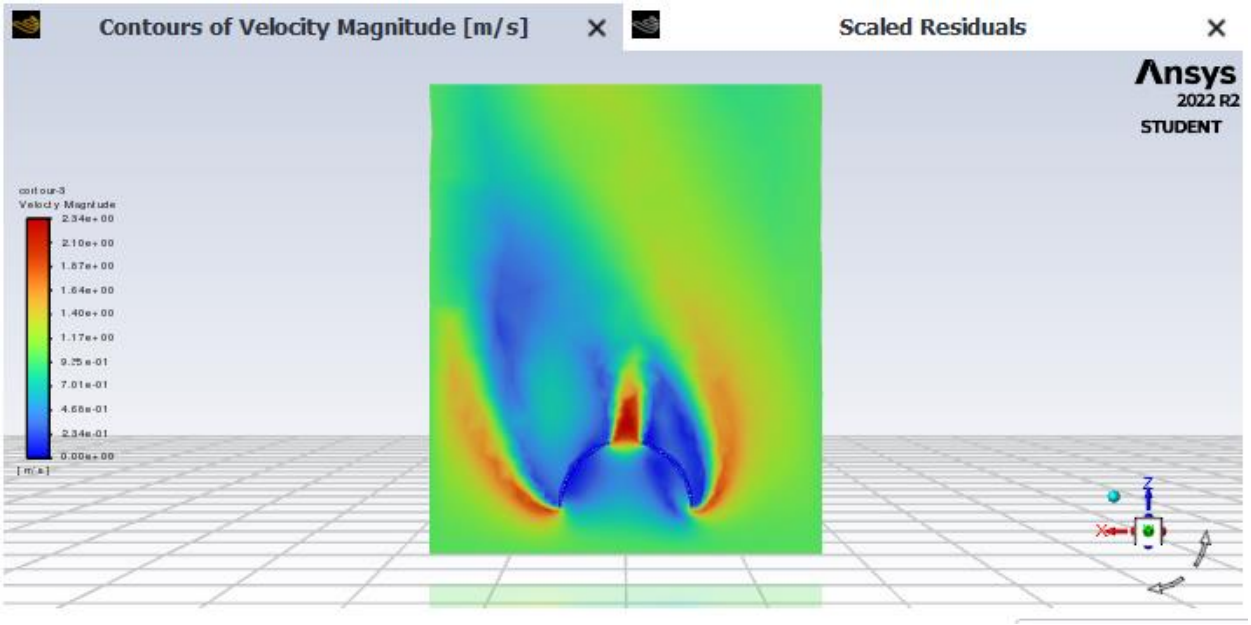

Fig. 11.4: Velocity contour of parachute tilted 15 degrees, hole size of 0.35m, falling at a terminal velocity of 1m/s

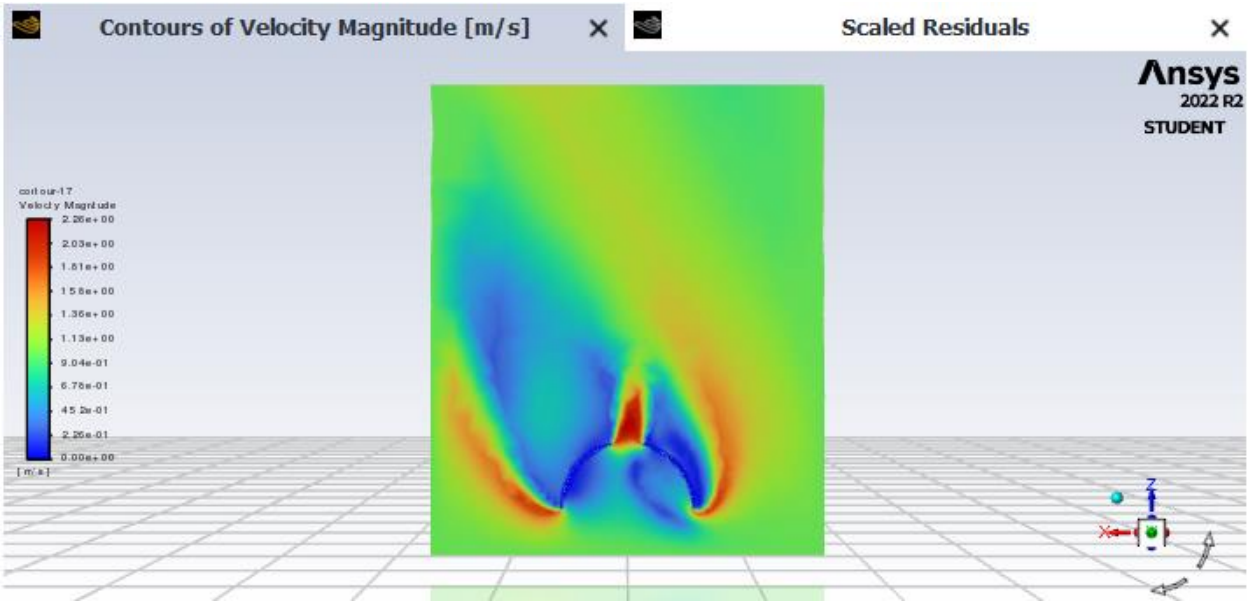

Fig. 11.5: Velocity contour of parachute tilted 20 degrees, hole size of 0.35m, falling at a terminal velocity of 1m/s

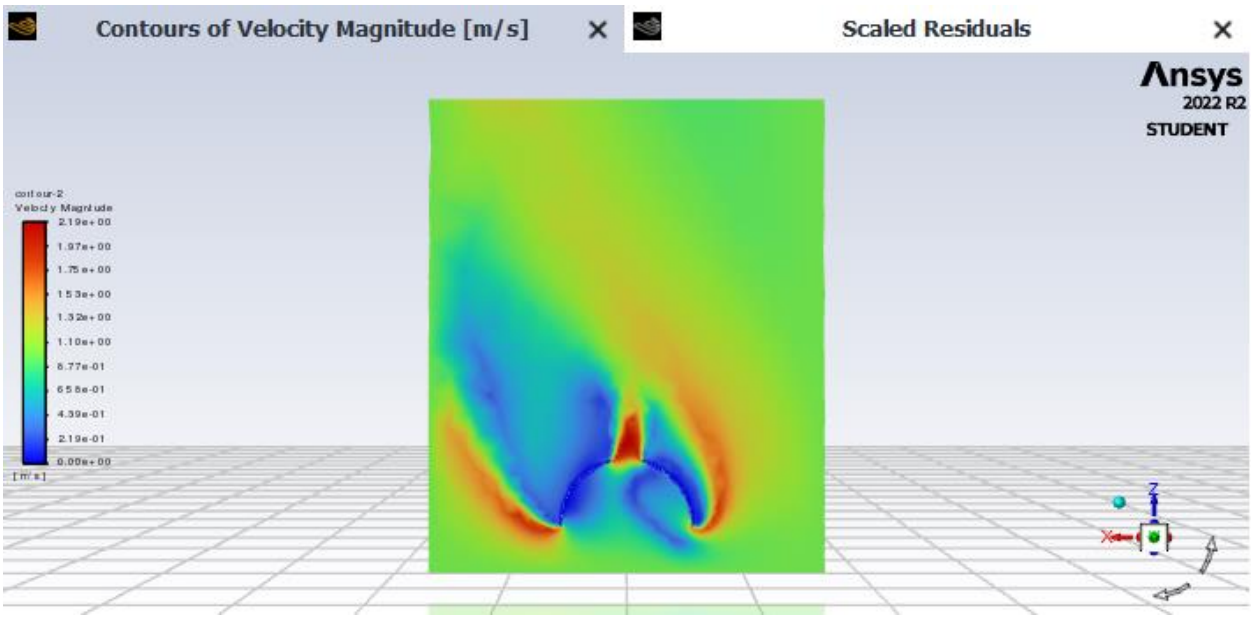

Fig. 11.6: Velocity contour of parachute tilted 25 degrees, hole size of 0.35m, falling at a terminal velocity of 1m/s

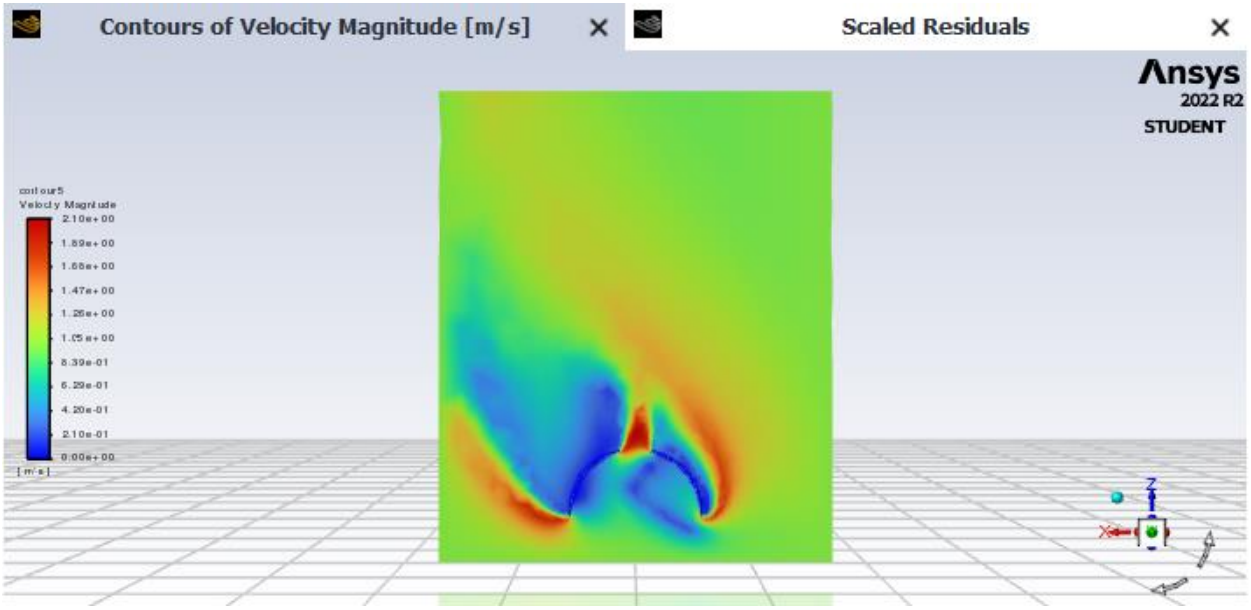

Fig. 11.7: Velocity contour of parachute tilted 30 degrees, hole size of 0.35m, falling at a terminal velocity of 1m/s

Fig 11.8: First Prototype

Fig 11.9: Second Prototype

Fig 11.10: Third Prototype

Fig 11.11: Final Prototype

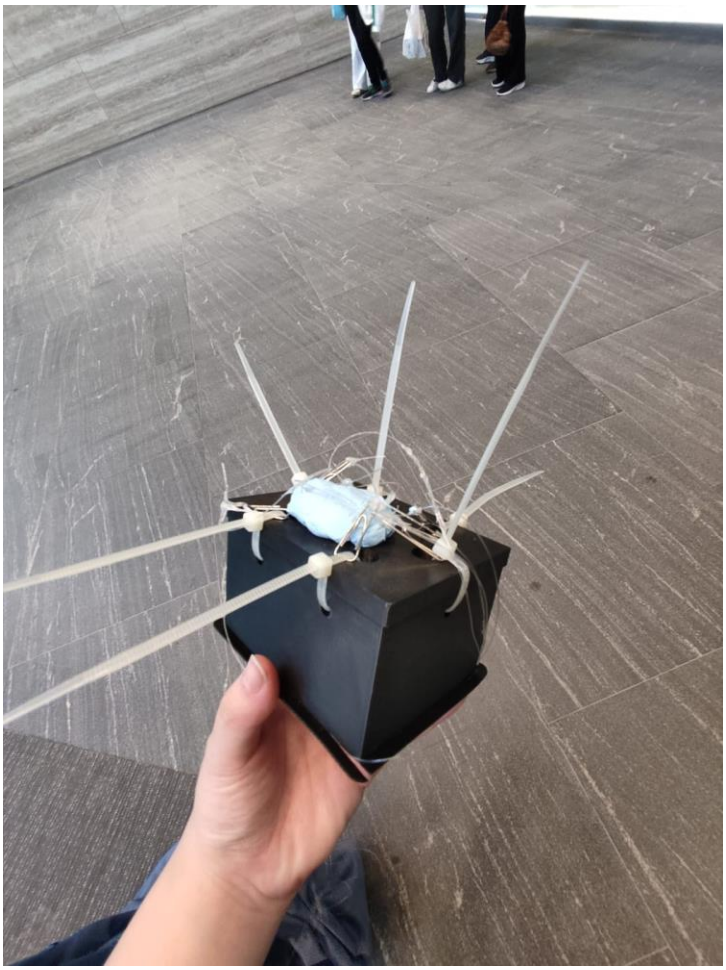

Fig 11.12: 3D Printed Box Payload